

The invariant manifolds and the Milky Way galactic bar(s)

M. Romero-Gómez¹, T. Antoja², F. Figueras¹, L.A. Aguilar³, and E. Athanassoula⁴

¹ Institut d'Estudis Espacials de Catalunya (IEEC), Institut de Ciències del Cosmos (ICC), Dept. Astronomia i Meteorologia, Universitat de Barcelona (UB), Martí i Franquès, 1, E08028 Barcelona, Spain

² Kapteyn Astronomical Institute, University of Groningen, PO Box 800, 9700 AV Groningen, the Netherlands

³ Instituto de Astronomía, Universidad Nacional Autónoma de México, Apdo. Postal 877, Ensenada, 22800, Baja California, México

⁴ Laboratoire d'Astrophysique de Marseille (LAM), UMR6110, CNRS/Université de Provence, Technopôle de Marseille Etoile, 38 rue Frédéric Joliot Curie, 13388 Marseille Cédex 20, France

Abstract

How many bars does the Milky Way have? This question has arisen due to recent results from theoretical models and N-body simulations. In this talk, firstly, we will present the results the invariant manifolds provide in this direction. We compute for the first time the galactic longitude - line-of-sight velocity diagram of orbits trapped by the manifolds in Galactic potentials with different configurations, namely one bar (the COBE/DIRBE bar) and two bars (the COBE/DIRBE and the Long bar misaligned). Secondly, we present the results from test particle simulations where the nonaxisymmetric component has one of the two configurations above. In particular, we study whether the kinematic structures in the Gaia sphere (4-5 kpc from the Sun) will be able to distinguish among the two cases.

1 Introduction

Whether the Milky Way has two bars with different angular separation or only one bar is a matter of debate in the literature. Observations detect a Long bar at an angle of $\sim 40^\circ$ from the Galactic Center - Sun line [6, 2, 8, 3]. On the other hand, the relative orientation of the COBE/DIRBE bar is not well established, although most observations (2MASS star counts or red clump giants) and models (based on COBE/DIRBE and Spitzer/GLIMPSE) agree it lies roughly within the range of $15^\circ - 30^\circ$ (e.g. [5] and references therein).

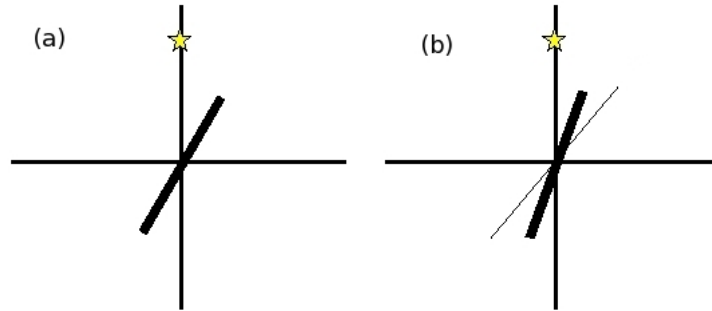


Figure 1: *Left panel (a)*: One bar configuration where the Galactic (thick solid line) is aligned at 20° from the Sun-Galactic Centre line. *Right panel (b)*: Two bars configuration where the Galactic bar lies at 20° from the Sun-Galactic Centre line and the Long bar, at 40° .

Numerical N-body simulations opt for the possibility that the Milky Way has only one bar with a boxy/bulge. And what COBE/DIRBE predicts as a Galactic bulge would correspond to the boxy/bulge of the bar and the long tip the observations predict is the long end of the bar [10, 9].

Here we propose two mechanisms to try to disentangle the controversy of the bar(s) of the Milky Way. In Sect. 2 we describe the two models used and in Sect. 3 we apply two different techniques to check whether they can help disentangling the nature of the bar component of the Milky Way.

2 Models

The two models used in this study are schematically shown in Fig. 1, namely case (a) has only the COBE/DIRBE bar, while case (b) has the COBE/DIRBE and the Long bar misaligned with an angular separation of 20° .

In both cases, the system is three dimensional. The axisymmetric component is fixed to the one in [1], to match the rotation curve of the Galaxy, and the non-axisymmetric component (one bar in case (a) and two bars in case (b)) is modelled using Ferrers ellipsoids. For the COBE/DIRBE bar, the semi-major axes are fixed to $3.13 : 1. : 1.$ kpc, and the mass is $9.8 \times 10^9 M_\odot$. The semi-major axis of the bar is at 30° from the Sun - Galactic Centre line. As for the Long bar, the three axes are set to $4.5 : 1.4 : 1.4$ kpc and the mass is set to $4.2 \times 10^9 M_\odot$. In this case, the COBE/DIRBE bar is at 20° and the Long bar, at 40° . In both cases, the non-axisymmetric component rotates as a solid rigid and in a constant pattern speed, $50 \text{ km s}^{-1} \text{ kpc}^{-1}$.

In all our plots, the Sun is located on the y-positive axis.

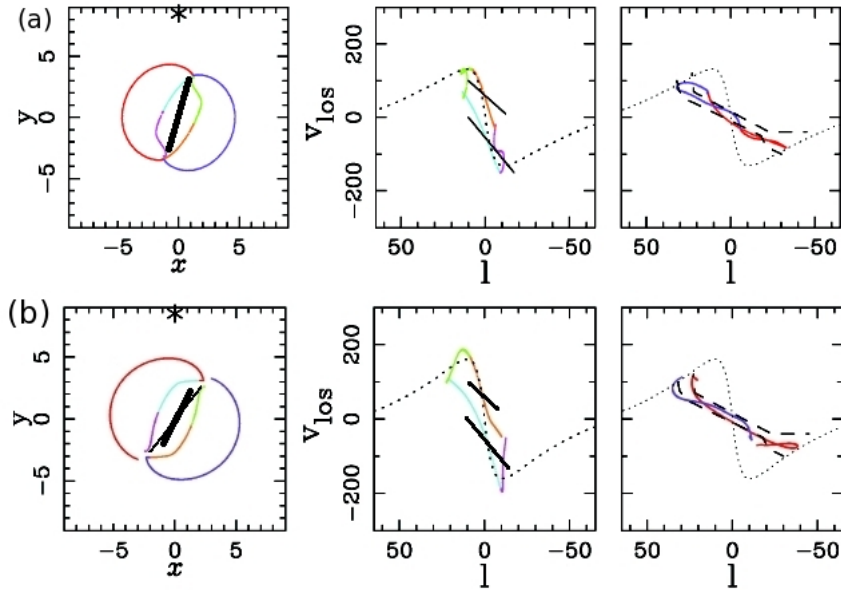


Figure 2: *Upper left panel (a)*: Orbits trapped by the manifolds in the one bar configuration. Different colours show different regions of the orbit. The solid thick line marks the position of the COBE/DIRBE bar. *Center and right panels (a)*: Line-of-sight velocity as a function of the galactic longitude for the inner (middle) and outer (right) orbits. The solid and dashed lines mark the position of the 3-kpc arms and the Galactic Molecular Ring, respectively. The dotted line is the terminal velocity curve. *Lower panels (b)*: As in panels (a) for the two bar configuration. The solid thin line in the left panel marks the position of the Long bar.

3 Disentangling the bar component

We perform two tests to try to disentangle the bar component of the Milky Way. The first consists of computing the invariant manifolds of the periodic orbits around the unstable equilibrium points and projecting them into the galactic longitude – line-of-sight velocity diagram. The second consists of running test particle simulations and checking the effect of the bar component on the kinematic (U, V) plane.

3.1 The invariant manifolds and the (l, v) diagram

This Section summarizes the results found in [10]. They are based on the dynamics around the equilibrium points. The ones along the bar semi-major axis are unstable saddle points. Each of them is surrounded by a family of unstable periodic orbits, so that any orbit in their immediate vicinity (in phase space) will have to escape the neighbourhood of the corresponding equilibrium point. The direction in which the orbit escapes is set by what we call the invariant manifolds. These can be thought of as tubes that guide the motion of particles of the same energy as the manifolds [7, 4]. In the left panels of Fig. 2, we show that from

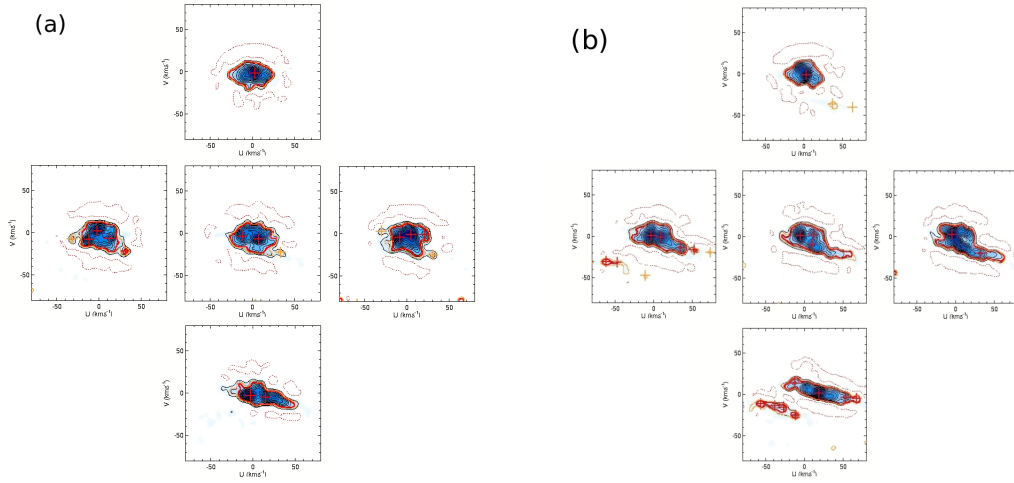


Figure 3: *Left panel (a)*: (U, V) planes for the one bar configuration. The central plane corresponds to the Solar neighbourhood. The plane below (above) correspond to regions towards (opposite) the Galactic centre, while the plane on the right (left) correspond to regions towards (opposite) the galactic rotation. *Right panel (b)*: Same as panel (a) for the two bar configuration.

each end of the bar emanate four branches: two of them inside corotation (inner branches light blue, green, orange and purple) and two of them outside it (outer branches, red and dark blue). Note that how in both cases the orbits delineate two rings, one more elongated reminding the 3-kpc arms and one more circular reminding the Galactic Molecular Ring.

In the middle and right panels, we project the orbits on the left panel into the galactic longitude - line-of-sight velocity diagram, hereafter (l, v) diagram. The dotted line shows the terminal velocity curve (directly related to the rotation velocity curve) and the solid (dashed) lines mark the position of the observed 3-kpc arm (Galactic Molecular Ring) in the (l, v) diagram.

Note how both rings fit well in the (l, v) diagram. However, the (l, v) diagram in both cases, namely one bar or two bars, are very similar so it seems that the (l, v) diagram does not help separating one configuration or another.

3.2 Test particle simulations and the (U, V) plane

In this second approach, we generate an ensemble of 2×10^7 particles following the Miyamoto-Nagai disc of the Allen & Santillán model of the Galaxy. They are given the kinematics of a “warm” population, i.e. $\sigma_U(R_\odot) = 20 \text{ km s}^{-1}$, $\sigma_V(R_\odot) = 15 \text{ km s}^{-1}$ and $\sigma_W(R_\odot) = 10 \text{ km s}^{-1}$, where $\sigma_U(R)$ is proportional to the surface density, $\sigma_V(R)$ is determined following the epicyclic approximation and $\sigma_W(R)$ is again proportional to the surface density and it assumes a constant scale-height. Then they are relaxed in the total Allen & Santillán axisymmetric potential (remember that it consists of a disc, a bulge and a halo). We introduce

the bar in 4 bar rotations and we let the particles adapt to the full potential another 2 rotations. In this final snapshot, we select five different regions of 1 kpc^2 . One is centered on the Sun and the other four are located at each side of the Sun neighbourhood. Towards and opposite the Galactic Centre and towards and opposite the galactic rotation. We compute the kinematic (U, V) plane in this five regions. Remember that the (U, V) is a galactocentric system, where the U component of the velocity points towards the Galactic Centre, while the V points towards the galactic rotation.

In Fig. 3, we show the wavelet transform of the (U, V) plane of the five regions mentioned above. The kinematic structures found have sizes between $6 - 13 \text{ km s}^{-1}$. The panels on the left are for the one bar configuration, while the panels on the right correspond to the two bars configuration. The red (orange) contour marks the 3σ (2σ) level while the red (orange) crosses mark the maxima found within the corresponding level. Note that the (U, V) planes change depending on the region under study, but also depending on the bar component.

4 Conclusions

We have used two different approaches to try to separate between two different configuration of the bar component of the Milky Way, namely the (l, v) diagram of the invariant manifolds and the (U, V) plane in different regions of the Galactic plane. We conclude that the (l, v) diagrams of the two cases are very similar, while the (U, V) planes show more differences between the two configurations in different regions of the Galactic plane.

Acknowledgments

This work was supported by the MINECO (Spanish Ministry of Economy) - FEDER through grant AYA2009-14648-C02-01 and CONSOLIDER CSD2007-00050.

References

- [1] Allen, C. & Santillán, A. 1991, *RevMexAA*, 22, 255
- [2] Benjamin, R.A., Churchwell, E., Babler, B.L., et al. 2005, *ApJ*, 630L, 149
- [3] Cabrera-Lavers, A., González-Fernández, C., Garzón, F., et al. 2008, *A&A*, 491, 781
- [4] Gómez, G., Koon, W.S., Lo, M. W., Marsden, J. E., et al. 2004, *Nonlinearity*, 17, 1571
- [5] Churchwell, E., Babler, B.L., Meade, M.R., et al. 2009, *PASP*, 121, 213
- [6] Hammersley, P.L., Garzón, F., Mahoney, T.J., et al. 2000, *MNRAS*, 317, L45
- [7] Koon, W. S. Lo, M. W., Marsden. J. E., & Ross, S. D. 2000, *Chaos*, 10, 2, 427
- [8] López-Corredoira, M., Cabrera-Lavers, A., Mahoney, T.J., et al. 2007, *AJ*, 133, 154
- [9] Martínez-Valpuesta, I. & Gerhard, O. 2011, *ApJ*, 734, L20
- [10] Romero-Gómez, M., Athanassoula, E., Antoja, T., & Figueras, F. 2011, *MNRAS*, 418, 1176